ELSEVIER

Coordination Chemistry Reviews
171 (1998) 387–398

COORDINATION CHEMISTRY REVIEWS

Emitting state energies and vibronic structure in the luminescence spectra of *trans*-dioxorhenium(V) complexes

Carole Savoie, Christian Reber *

Département de chimie, Université de Montréal, C.P. 6128, Succ. Centre-ville, Montréal, Qué. H3C 3J7, Canada

Received 7 July 1997; received in revised form 15 August 1997; accepted 19 November 1997

Contents

Abstract

The luminescence properties of a series of *trans*-dioxo complexes of rhenium(V) with nitrogen donor ligands are summarized and their luminescence spectra analyzed. New emissions in the visible to near infrared wavelength region are observed for dioxo complexes with imidazole and ethylenediamine ligands. The intensity distribution within the main progression of the resolved spectra is very similar for all compounds, despite a variation of the luminescence band maxima by approximately 3000 cm^{-1} within the series of complexes. Molecular orbital and crystal field models are combined with time-dependent theory to analyze the experimental results. Unusual vibronic structure is shown to arise from coupling between the $^1A_{1g}$ (D_{4h} point group) ground state and a $^1A_{1g}$ excited state, an effect that is correlated with excited state energies. © 1998 Elsevier Science S.A.

Keywords: Metal-oxo complexes; Near-infrared luminescence; Vibronic structure

1. Introduction

Trans-dioxo complexes of rhenium(V) are a well-known category of transition metal compounds with metal–ligand multiple bonds [1]. Their spectroscopic and

* Corresponding author. Fax: +1 514 343 7586; e-mail: reber@chimie.umontreal.ca

PII S0010-8545(98)00015-0

photochemical properties have been summarized in a number of recent reviews and books [2–4]. Some of these complexes show luminescence in the visible region. A representative example is $ReO_2(py)_4^+$ with a structured emission band between 590 nm and 750 nm [5]. Luminescence from isoelectronic *trans*-dioxoosmium(VI) complexes is usually observed in a similar wavelength range, illustrated by *trans*-$OsO_2(CN)_4^{2-}$ which emits between 615 nm and 800 nm [6,7].

We present and analyze luminescence spectra of a series of *trans*-dioxorhenium(V) complexes with emitting states at lower energy than the examples given above, i.e. in the visible to near-infrared (NIR) borderline wavelength range between 700 nm and 1150 nm [8]. The factors leading to low-energy emitting states are identified from the comparison of experimental spectra with molecular orbital calculations and with a recent crystal field model [4]. These electronic models are combined with time-dependent theory [9–11] to calculate emission spectra, allowing for a detailed analysis of the resolved vibronic structure. The observed variations of emitting state energies and the resolved vibronic structure are reproduced by our approach, and we obtain quantitative bond length changes of the emitting state. The analysis also provides insight into the physical origin of the unusual vibronic structure observed in *trans*-dioxorhenium(V) complexes with particularly low-energy emitting states [8].

2. Summary of spectroscopic results

The instrumentation and data acquisition procedures used for our spectroscopic measurements have been described in detail elsewhere [12,13]. Onsets and maxima of the luminescence bands for a series of complexes studied in our laboratory are summarized in Table 1 and compared to selected examples from the literature. An extensive summary of spectroscopic data for other d^2 *trans*-MO_2L_4 complexes is presented in ref. [4].

Fig. 1 shows single-crystal low-temperature luminescence spectra of two new *trans*-$MO_2L_4^+$ complexes, where L denotes vinylimidazole and 1-methylimidazole. Luminescence is observed between 14500 cm^{-1} and 9000 cm^{-1}, lower in energy by approximately 2500 cm^{-1} than the emission from the pyridine analog [5]. Both spectra in Fig. 1 show resolved vibronic structure with a dominant progression in the totally symmetrical O=Re=O stretching mode with frequencies between 880 cm^{-1} and 905 cm^{-1} as shown in Table 1. The vibrational energies observed in Raman spectra and in the luminescence progression are in excellent agreement. Each member of this progression consists of a cluster of bands corresponding to a second progression in a lower energy mode, most likely involving the four imidazole ligands of the complexes in Fig. 1. This mode has a frequency of approximately 200 cm^{-1}, a region where vibrational spectra show a large number of bands. The low-frequency vibration cannot be unambiguously assigned to a specific metal–ligand mode. The luminescence onset is 400 cm^{-1} higher in energy for the vinylimidazole complex than for the 1-methylimidazole compound, a significant change caused by the different substitution on the nitrogen donor ligand.

The onsets of absorption and luminescence spectra coincide, indicating emission

Table 1
Summary of luminescence properties of *trans*-ReO_2L_4 complexes

L, X in *trans*-$[ReO_2L_4]X$	E_0^a, lumin. (cm^{-1})	E_{max}, lumin. (cm^{-1})	$\hbar\omega_{O=Re=O}$ (cm^{-1})	$\hbar\omega_{Re-N}$ (cm^{-1})	$\Delta r_{Re=O}$ (Å)	k_c (cm^{-1})
2-Ethyl-4-methylimidazole, BPh_4^-	13200	11200				
Isopropylimidazole, I^-	13600	11000				
Ethylenediamine, Cl^-	14200	12190	880 899[b]	210	0.09	6
1-Methylimidazole, I^-	14300	12710	905 905[b]	200	0.08	11
1-Methylimidazole, BPh_4^-	14500	13100	890	200		
1,2-Dimethylimidazole, I^-	13900	12730	890	200	0.07	
Vinylimidazole, I^-	14700	13310	885	210	0.07	2
Tetramethylethylenediamine, Cl^-	17660	15910	890	200	0.08	3
Tetraethylethylenediamine, BPh_4^-		17500				
Pyridine, BPh_4^-[c]	16680	15400	900	190	0.07	≈0
CN^-, K^+[c]	17800	16700	900		0.09	

[a] Electronic origin.
[b] Raman.
[c] Ref. [5].

from the majority chromophore in the crystals [8]. Some absorption spectra show resolved vibronic structure on the lowest energy band, allowing us to estimate the change in O=Re=O vibrational frequency between the ground and emitting states. These values are included in Table 1. The Stokes shift for *trans*-ReO_2(1-methylimidazole)$_4^+$ is 2900 cm^{-1}, indicating a significant structural change between the ground and emitting states.

The luminescence lifetimes for complexes with low-energy emission bands are shorter by more than an order of magnitude than radiative lifetimes estimated from oscillator strengths. The low-temperature lifetime for *trans*-ReO_2(1-methylimidazole)$_4^+$ is only 1.6 μs at 6 K, for the pyridine analog it is 68 μs [5]. This difference indicates that non-radiative relaxation processes become more efficient in molecules with low-energy emitting states, a qualitative trend that has been reported for many transition metal luminophores [14].

3. Discussion

3.1. Emitting state energies

Rhenium(V) has the $[Xe]5d^2$ electron configuration. We use the D_{4h} point group throughout this analysis of *trans*-MO_2L_4 complexes as an approximation to the actual molecular symmetry, which is often much lower [15,16]. The electronic spectra are close to those expected for D_{4h} symmetry, indicating that the structural deviations have only a minor effect on the energy of electronic states and on the spectra. In the following, we choose the molecular z axis to coincide with the

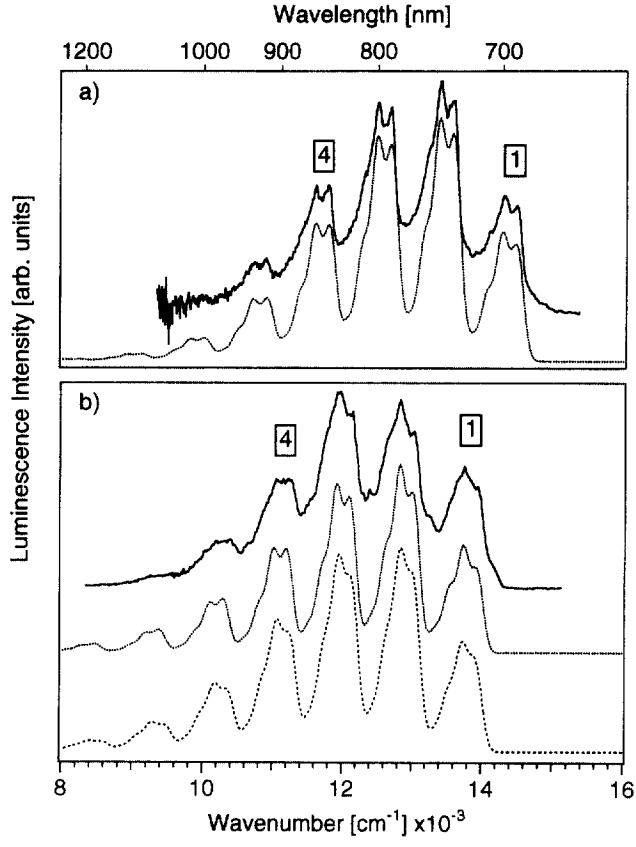

Fig. 1. Single-crystal luminescence spectra of (a) *trans*-ReO_2(vinylimidazole)$_4$I (6 K) and (b) *trans*-ReO_2(1-methylimidazole)$_4$I (15 K). Calculated spectra are shown as dotted lines, the bottom trace in (b) denotes the calculated spectrum for purely harmonic surfaces.

metal–oxo double bonds, as shown in Fig. 2. The nitrogen donor ligands are located in the *xy* plane. The d-orbitals are split into b_{2g} (d_{xy}), e_g (d_{xz}, d_{yz}), b_{1g} ($d_{x^2-y^2}$) and a_{1g} (d_{z^2}), as indicated in the qualitative orbital energy level diagram in Fig. 2. The lowest energy electronic transition in *trans*-dioxo complexes corresponds to a $d_{xy} \rightarrow d_{xz,yz}$ orbital excitation and occurs between the $^1A_{1g}$ ground state and the ^3E_g and ^1E_g excited states, leading to a spin-forbidden and a spin-allowed d–d band, observed in the absorption spectra of many complexes [5]. The emitting level is therefore a component of the ^3E_g state, split by spin–orbit coupling and the low actual symmetry.

An alternative confirmation of the assignment of the lowest excited electronic states is obtained from a comparison of the observed vibrational frequencies for both the ground and emitting states. We use the experimental values for *trans*-ReO_2(ethylenediamine)$_2^+$ as an example for this comparison. The vibrational frequencies of the O=Re=O and the Re–(en)$_2$ modes in the ground state are

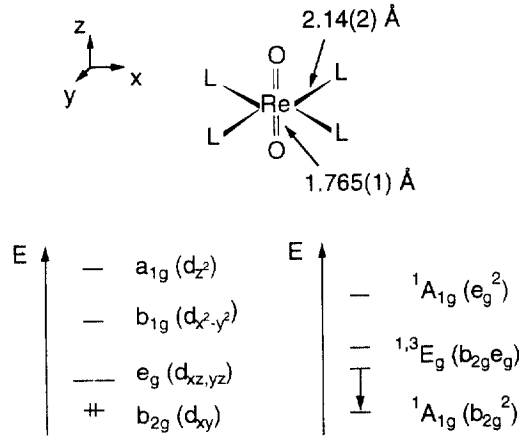

Fig. 2. Schematic structure and definition of molecular axes for *trans*-dioxorhenium(V) complexes. Bond lengths are average values for the compounds in Fig. 3(a)–(c) with L denoting 1-methylimidazole, pyridine and ethylenediamine. The qualitative splitting of the 5d orbitals in idealized D_{4h} symmetry and the low-energy electronic states with their orbital configurations are given. The arrow denotes the luminescence transition.

determined from the luminescence spectrum as 880 cm^{-1} and 210 cm^{-1} [17]. The resolved absorption spectrum leads to frequencies for the excited state of 795 cm^{-1} and 260 cm^{-1} for the two vibrational modes [5,17]. The metal–oxo frequency decreases in the emitting state, as expected for the $b_{2g}e_g$ electron configuration with its larger metal–oxo π antibonding character than the $(b_{2g})^2$ configuration of the ground state. The rhenium–ethylenediamine vibrational frequency increases in the excited state because an electron is removed from the somewhat metal–nitrogen antibonding d_{xy} orbital. The observed vibrational frequencies confirm therefore the energetic order of orbitals giving rise to the ground and lowest energy excited states.

The energies of the luminescence band maxima in Table 1 vary significantly within the series of ligands studied. One of the important parameters determining these transition energies is the energy difference between the d_{xy} and $d_{xz,yz}$ orbitals. Extended Hückel molecular orbital (EHMO) calculations [18] based on the crystal structures of ReO_2(1-methylimidazole)$_4^+$, ReO_2(pyridine)$_4^+$ and ReO_2(ethylenediamine)$_2^+$ [15,16] are used to examine orbital energies and to compare them to the observed variation of the luminescence energies. Average rhenium–oxo distances are 1.766 Å, 1.764 Å and 1.765 Å, and average rhenium–nitrogen distances are 2.121 Å, 2.148 Å and 2.162 Å for the three complexes, illustrating their structural similarity. The energies of the HOMO (b_{2g}, predominantly d_{xy}) and LUMO (e_g, predominantly $d_{xz,yz}$) orbitals are shown in the middle columns of Fig. 3(a)–(c) and compared to the ReO_2 and nitrogen donor orbital energies for every complex.

The LUMO orbitals are at similar energies for all three compounds and we note that the splitting of the e_g orbitals due to lower site symmetry is smaller than 200 cm^{-1}, further justifying our idealized D_{4h} point group. The HOMO–LUMO energy gaps are denoted as Δ_π in Fig. 3. Their numerical values are

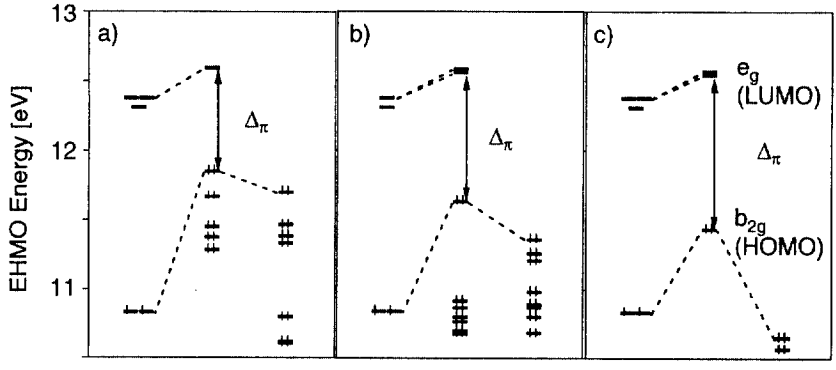

Fig. 3. EHMO energy levels for (a) *trans*-ReO_2(1-methylimidazole)$_4^+$, (b) *trans*-ReO_2(pyridine)$_4^+$ and (c) *trans*-ReO_2(ethylenediamine)$_2^+$. The crystal structures of the complexes were used in the calculations. Fragment molecular orbital diagrams are constructed from the ReO_2 unit (left) and the nitrogen ligands (right).

5960 cm^{-1}, 7400 cm^{-1} and 8900 cm^{-1} for the 1-methylimidazole, pyridine and ethylenediamine complexes, respectively. This variation is caused by the destabilization of the HOMO orbital due to π antibonding interactions with the nitrogen donor ligands, an effect that is most important for imidazole, less important for pyridine and least important for saturated ligands such as ethylenediamine. The calculated HOMO–LUMO energy differences predict higher energy emission from the pyridine complex than from the imidazole compound, in qualitative agreement with the experimental observation. The origin of the difference is identified as the HOMO energy. From the orbital energies in Fig. 3 we expect the highest energy emission to occur from ReO_2(ethylenediamine)$_2^+$, which is clearly not the case according to Table 1. Luminescence from the ethylenediamine complex is observed in an energy range similar to the imidazole compounds in Fig. 1. The molecular orbital model is therefore not able to rationalize all observed luminescence energies.

The luminescence band widths and resulting Re=O bond length changes in the emitting state of the *trans*-dioxo complexes are almost identical, despite the large variation of the emission band maxima summarized in Table 1. This observation can be rationalized with the orbital energy levels in Fig. 3. The spectra in Fig. 1 and many similar examples in the literature show that luminescence band shapes of *trans*-dioxorhenium complexes are dominated by the intensity distribution within the high-frequency progression. This intensity distribution is a result of the structural change between the ground and excited states along the totally symmetric O=Re=O normal coordinate Q_{Re-O}. The most important reason for this structural change is the metal–oxo antibonding character of the e_g orbitals, occupied only in the emitting state. These orbitals are destabilized to almost identical energies for all compounds in Fig. 3, and their identical antibonding character leads to similar Re=O bond length changes. In contrast, it is the energy of the HOMO orbital that is responsible for the change in emission energy. This orbital has a negligible effect on the Re=O

bonds. We note that simple relations [19] linking excited state distortions and electronic transition energies should not be applied to the title compounds.

A model allowing a more complete analysis of the trends in emitting state energies for the complexes in Table 1 has to include electron–electron interactions. We use the crystal field model and formalism presented in ref. [4]. The difference between the b_{2g} and e_g orbitals is denoted as Δ_π, as illustrated in Fig. 3, and the interelectronic repulsion is represented by the parameter K_{xy}, defined in terms of the Racah parameters as [4]:

$$K_{xy} = 3B + C \quad (1)$$

The low-energy electronic states of interest arise from the $(b_{2g})^2$, $b_{2g}e_g$ and $(e_g)^2$ electron configurations, as indicated in Fig. 2. They are shown in Fig. 4 as a function of Δ_π for two values of K_{xy}. We include the labels for the states in O_h symmetry, corresponding to $\Delta_\pi = 0$, to illustrate the relationship of the states in Fig. 4 to those found in a standard Tanabe–Sugano diagrams for the d^2 configuration.

We concentrate in the following on the $^1A_{1g}$ ground state and the ^3E_g emitting state. The separation between the ^1E_g and ^3E_g states is $2K_{xy}$ in our model. The experimental energy difference between the two d–d absorption bands should only very cautiously be used to determine K_{xy} because it also depends on spin–orbit coupling and possibly on Jahn–Teller stabilization energies [4]. We neglect spin–orbit

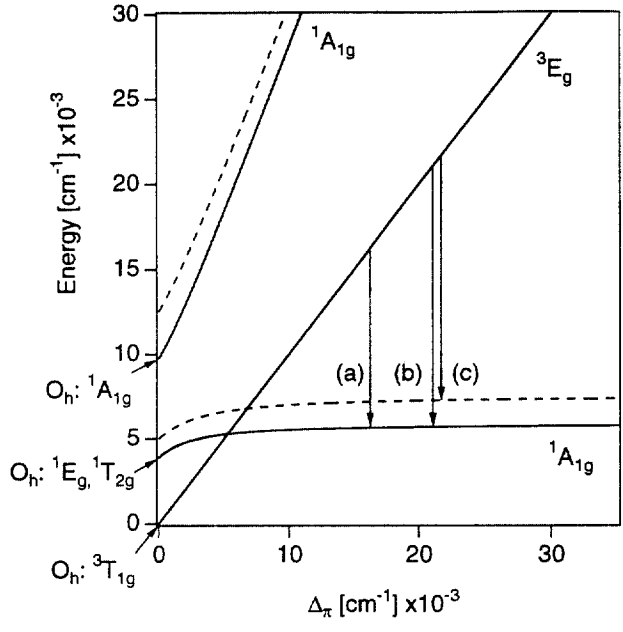

Fig. 4. Electronic states for *trans*-dioxorhenium(V) complexes with the d^2 electron configuration as a function of Δ_π for $K_{xy} = 1950\ cm^{-1}$ (solid lines) and $K_{xy} = 2500\ cm^{-1}$ (dotted lines). Arrows labeled (a), (b) and (c) denote luminescence maxima for *trans*-ReO_2(1-methylimidazole)$_4^+$, *trans*-ReO_2(pyridine)$_4^+$ and *trans*-ReO_2(ethylenediamine)$_2^+$, respectively.

coupling in our analysis because it does not split the ground state. The ground state energy depends on both Δ_π and K_{xy}. The off-diagonal matrix element with the $^1A_{1g}$ state arising from the $(e_g)^2$ configuration, calculated in ref. [4] as $\sqrt{2}K_{xy}$, has to be taken into account. The ground state energy is given by:

$$E(^1A_{1g}) = \frac{7K_{xy} + 2\Delta_\pi - \sqrt{(-7K_{xy} - 2\Delta_\pi)^2 - 4K_{xy}(10K_{xy} + 6\Delta_\pi)}}{2} \quad (2)$$

The energy of the ^3E_g excited state is:

$$E(^3E_g) = \Delta_\pi \quad (3)$$

Fig. 4 shows the energies of the relevant electronic states as a function of Δ_π for two values of K_{xy}, one of them the value of 1950 cm^{-1} for K_{xy} determined for the pyridine complex [4,5]. The energy difference between the ground and emitting states increases with Δ_π. In the preceding section and in Fig. 3 we show that Δ_π for the imidazole complex is smaller than for the pyridine complex. Fig. 4 therefore rationalizes the observed order of $^1A_{1g} \leftrightarrow {}^3E_g$ transition energies for these compounds.

The difference between the ground and emitting states and therefore the emission energy also depends on K_{xy}, as illustrated in Fig. 4. Based on the nephelauxetic series, we expect a higher value of K_{xy} for the ethylenediamine complex than for the aromatic pyridine and imidazole ligands. An increase of this parameter to 2500 cm^{-1} decreases the emission energy by 1500 cm^{-1}, a reduction of the emission energy corresponding approximately to the difference between pyridine and ethylenediamine. A similar effect contributes to the large difference in emission energy between the ethylenediamine and the tetramethylethylenediamine complexes. The interelectronic repulsion parameters B and C were found to decrease in a series of tetragonal $Ni(NCS)_2L_2$ complexes if L is varied from ethylenediamine to tetramethylethylenediamine and to tetraethylethylenediamine [20,21]. The reduction of K_{xy} is therefore an important element contributing to the increase of the emission energy observed for the substituted ethylenediamine complexes. The crystal field model reproduces the trends in emitting state energy observed for all nitrogen donor ligands in Table 1.

3.2. *Vibronic structure in the luminescence spectra*

The resolved vibronic structure in the luminescence spectra in Fig. 1 provides the experimental information necessary for a quantitative characterization of the emitting state geometry. The luminescence band shape arises from progressions in two modes whose vibrational energies differ by more than a factor of four, as indicated in Table 1. Detailed vibronic effects in both modes can therefore be observed separately, a unique opportunity for a detailed comparison of theoretical models with experimental spectra. For uncoupled, purely harmonic modes we expect each member of the high-frequency progression to consist of an identically shaped cluster of peaks separated by the low vibrational frequency. In order to quantitatively compare such a prediction with the experimental spectrum, we include a calculated spectrum based

on two-dimensional harmonic oscillator potentials in Fig. 1(b). We use the time-dependent theory of spectroscopy [9–11] to calculate spectra from different potential energy surfaces.

The two-dimensional harmonic oscillator potential energy surfaces for the electronic ground state and the emitting state are given by Eqs. (4) and (5). Dimensionless normal coordinates $Q_{\text{Re–O}}$ and $Q_{\text{Re–N}}$ represent the two vibrational modes observed in the luminescence spectrum:

$$V_{\text{harm,gs}}(Q_{\text{Re–O}}, Q_{\text{Re–N}}) = \tfrac{1}{2}\hbar\omega_{\text{Re–O}} Q^2_{\text{Re–O}} + \tfrac{1}{2}\hbar\omega_{\text{Re–N}} Q^2_{\text{Re–N}} \tag{4}$$

$$V_{\text{harm,es}}(Q_{\text{Re–O}}, Q_{\text{Re–N}}) = \tfrac{1}{2}\hbar\omega_{\text{Re–O}}(Q_{\text{Re–O}} + \Delta Q_{\text{Re–O}})^2 + \tfrac{1}{2}\hbar\omega_{\text{Re–N}}(Q_{\text{Re–N}} + \Delta Q_{\text{Re–N}})^2 + E_0 \tag{5}$$

Numerical values for the electronic origin E_0 and for the vibrational energies $\hbar\omega_{\text{Re–O}}$, $\hbar\omega_{\text{Re–N}}$, $\hbar\omega'_{\text{Re–O}}$ and $\hbar\omega'_{\text{Re–N}}$ were determined directly from the experimental luminescence and absorption spectra. The differences ΔQ along the dimensionless Re–O and Re–N normal coordinates are adjustable parameters that were used to calculate the bond length changes $\Delta r_{\text{Re–O}}$ given in Table 1 as described in detail in ref. [8].

The main discrepancy between the experimental and calculated spectra based on harmonic potentials in Fig. 1(a) concerns the shape of the members of the main progression. The clusters labeled 1 and 4 in Fig. 1 have exactly the same shape in the calculated spectrum, but their shapes are not identical in the experimental spectrum.

The origin of this particular vibronic effect is qualitatively illustrated in Fig. 5. The ground state potential energy surface is coupled to the surface of the $^1A_{1g}$ state arising from the $(e_g)^2$ electron configuration. This coupling is mediated by the off diagonal matrix element depending on the interelectronic repulsion parameter K_{xy}. The curvature of the adiabatic ground state potential energy surface varies along the abscissa of Fig. 5, an important deviation from a purely harmonic model. The shape of the potential energy surface is determined by the energy difference between the two $^1A_{1g}$ states, their vibrational frequencies and the offset of the excited $^1A_{1g}$ state along the two normal coordinates. The d–d transition to the high-energy $^1A_{1g}$ state is expected to be weak because it corresponds to a two-electron transition in the strong-field limit [22]. It is hidden in the absorption spectrum below more intense charge-transfer bands. We have therefore not nearly enough experimental information to determine all parameters that define the ground state potential energy surface in Fig. 5. The coupling constant used in Fig. 5 was calculated from the estimated K_{xy} values derived in the previous section and assumed to be identical for the two complexes.

We define a simplified model for the ground state potential energy surface which retains as its most important aspect a variable curvature of the potential along the $Q_{\text{Re–O}}$ coordinate, qualitatively similar to the ground state surface in Fig. 5:

$$V_{\text{gs}}(Q_{\text{Re–O}}, Q_{\text{Re–N}}) = V_{\text{harm,gs}}(Q_{\text{Re–O}}, Q_{\text{Re–N}}) + k_c Q^2_{\text{Re–O}} Q_{\text{Re–N}} \tag{6}$$

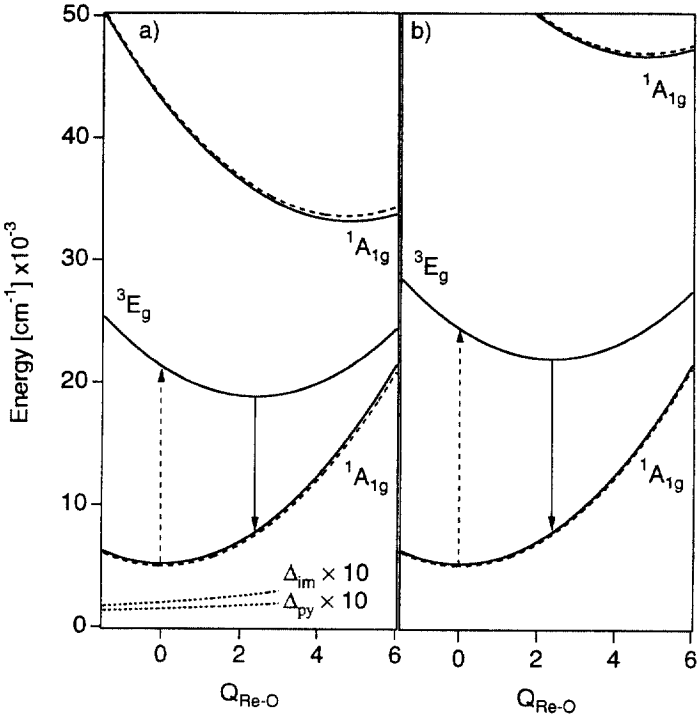

Fig. 5. Potential energy surfaces along the O=Re=O symmetrical stretching normal coordinate Q_{Re-O} for (a) *trans*-ReO_2(1-methylimidazole)$_4^+$ and (b) *trans*-ReO_2(pyridine)$_4^+$. Absorption transitions are given as dotted arrows, their energies correspond to the differences between the electronic states in Fig. 4. Emission transitions are shown as solid arrows. Dotted lines denote adiabatic potential energy surfaces for the two complexes. Difference traces between the diabatic (harmonic) and adiabatic potentials are enlarged by a factor of 10, and are denoted as Δ_{im} and Δ_{py} for the 1-methylimidazole and pyridine complexes, respectively.

This equation reduces the effect of coupling to a single parameter, k_c, instead of the three unknown parameters and the estimated value of K_{xy} required for a full description of the ground state surface. Graphical representations of this type of potential energy surface are available in the literature [11,23]. The calculated spectra obtained using the ground state potential energy surface in Eq. (6) are compared to experimental luminescence spectra of two ReO_2(imidazole)$_4^+$ complexes in Fig. 1. These calculated emission spectra are in better agreement with the experimental data than the uncoupled harmonic calculation, illustrated by a comparison of the clusters 1 and 4 in Fig. 1. All the parameters in Eq. (6) were held fixed at the values determined for the uncoupled harmonic model, and values of 11 cm^{-1} [8] and 2 cm^{-1} were obtained for k_c in the 1-methylimidazole and vinylimidazole complexes, respectively.

The coupling constants k_c for the imidazole complexes decrease with increasing luminescence energy. This trend is confirmed by the literature spectrum for

$ReO_2(pyridine)_4^+$, which emits at higher energy and shows no evidence for coupling. All members of the progression in the high-frequency mode have exactly the same shape and therefore k_c is negligible for this complex [5]. A qualitative explanation for this trend can be derived from a comparison of Fig. 5(a) and (b). We note that the ground state potential energy surface for the imidazole complex deviates more from the harmonic model than the surface of the pyridine complex, a consequence of the larger offset of the two coupled $^1A_{1g}$ surfaces along the energy axes for the pyridine complex. Traces denoting this difference are included in Fig. 5(a). The unusual variation of the vibronic structure is therefore a direct consequence of the coupling between the ground state and a high-energy excited state of the same symmetry.

The title compounds show detailed electronic spectra that allow us to gain new insight into the importance of several factors determining excited state energies and bond length changes in the excited state. The trends presented and analyzed with our examples can be used in the rational search for complexes with designed luminescence properties.

Acknowledgements

This work was made possible by research grants from the NSERC (Canada). We thank Andreea Vuica for help with the luminescence spectroscopy of some *trans*-dioxo complexes during her undergraduate summer research project.

References

[1] W.A. Nugent, J.M. Mayer, Metal–Ligand Multiple Bonds, Wiley, New York, 1988 and references cited therein.
[2] V.W.-W. Yam, C.-M. Che, Coord. Chem. Rev. 97 (1990) 93 and references cited therein
[3] D.M. Roundhill, Photochemistry and Photophysics of Metal Complexes, Plenum Press, New York, 1994 and references cited therein.
[4] V.M. Miskowski, H.B. Gray, M.D. Hopkins, in: C.-M. Che, V.W.-W. Yam (Eds.), Advances in Transition Metal Coordination Chemistry, Vol. 1, JAI Press, Greenwich, CT, 1996, p. 159 and references cited therein.
[5] J.R. Winkler, H.B. Gray, Inorg. Chem. 24 (1985) 346.
[6] C.-M. Che, V.W.-W. Yam, K.-C. Cho, H.B. Gray, Chem. Commun. (1987) 948.
[7] C. Sartori, W. Preetz, Z. Naturforsch. 43a (1988) 239.
[8] C. Savoie, C. Reber, S. Bélanger, A.L. Beauchamp, Inorg. Chem. 34 (1995) 3851.
[9] E.J. Heller, Acc. Chem. Res. 14 (1981) 368.
[10] J.I. Zink, K.-S. Kim Shin, in: D.H. Volman, G.S. Hammond, D.C. Neckers (Eds.), Advances in Photochemistry, Vol. 16, Wiley, New York, 1991, p. 119.
[11] D. Wexler, J.I. Zink, C. Reber, in: H. Yersin (Ed.), Electronic and Vibronic Spectra of Transition Metal Complexes I, Topics in Current Chemistry Series, Vol. 171, Springer, Berlin, 1994, p. 173.
[12] M.J. Davis, C. Reber, Inorg. Chem. 34 (1995) 4585.
[13] U. Oetliker, C. Reber, J. Near Infrared Spectrosc. 3 (1995) 63.
[14] C. Reber, H.U. Güdel, J. Lumin. 47 (1990) 7.
[15] C.J.L. Lock, G. Turner, Acta Crystallogr. B34 (1978) 923.

[16] S. Bélanger, A.L. Beauchamp, Inorg. Chem. 35 (1996) 7836.
[17] C. Savoie, C. Reber, in preparation.
[18] G. Landrum, Yet another extended Hückel molecular orbital package (YAeHMOP), version 2.0, available at http://overlap.chem.cornell.edu:8080/yaehmop.html., Cornell University, 1997.
[19] M.A. Hitchman, Inorg. Chem. 21 (1981) 821.
[20] A.B.P. Lever, G. London, P.J. McCarthy, Can. J. Chem. 55 (1977) 3172.
[21] A.B.P. Lever, I.M. Walker, P.J. McCarthy, K.B. Mertes, A. Jircitano, R. Sheldon, Inorg. Chem. 22 (1983) 2252.
[22] S.F.A. Kettle, Physical Inorganic Chemistry, University Science Books, Sausalito, CA. 1996, p. 175.
[23] D.J. Tannor, J. Phys. Chem. 92 (1988) 3341.